[22] C. Pecharroman, J. S. Moya, *Adv. Mater.* **2000**, *12*, 294.
[23] C. Pecharroman, E. B. Fatima, J. S. Moya, *Adv. Mater.* **2001**, *13*, 1541.
[24] D. M. Grannan, J. C. Garland, D. B. Tanner, *Phys. Rev. Lett.* **1981**, *46*, 375.
[25] D. J. Bergman, *Phys. Rev. Lett.* **1980**, *44*, 1285.
[26] Y. Meir, *Phys. Rev. Lett.* **1999**, *83*, 3506.
[27] C. Chiteme, D. S. Mclachlan, *Phys. B* **2000**, *279*, 69.
[28] R. Mezzenga, J. Ruokolainen, G. H. Fredrickson, E. J. Kramer, D. Moses, A. J. Heeger, O. Ikkala, *Science* **2003**, *299*, 1872.

Morphological Control of Tapered and Multi-Junctioned Carbon Tubular Structures**

By *Gopinath Bhimarasetti*, *Mahendra K. Sunkara*,* *Uschi M. Graham*, *Burton H. Davis*, *Changwon Suh*, and *Krishna Rajan*

The myriad structural manifestations and their material properties have made carbon nanostructures very interesting not only for potential applications but also for understanding carbon at the atomic scale. Several different nano-sized structures of carbon have been investigated intensely. A few of these include single and multi-walled nanotubes,[1] helical nanotubes,[2] cones,[3] horns,[4] conical crystals,[5,6] microtrees,[7] and nanopipettes.[8] The synthesis methods for carbon tubes with larger inner diameters are of interest for applications in micro-/nano-fluidics. Libera and Gogotsi[9] reported hydrothermal synthesis of graphite tubes with higher inner diameters ranging from 70–1300 nm using nickel as a catalyst. They also found that the tubes encapsulated "hydrothermal fluid" and process gases during the growth with a fraction of the tubes also containing inner obstructions reminiscent of bamboo styling due to nickel catalyst. Bando and co-workers[10,11] synthesized gallium-filled straight nanotubes using thermal evaporation of gallium oxide mixed with carbon. Similar results were obtained with thermal evaporation of gallium nitride powder in the presence of acetylene.[12] These gallium-filled straight carbon tubes have been projected as nano-thermometers. Here, we describe a method for synthesis of new types of morphologies for carbon tubular structures based on varying inner diameter. It is shown that these new morphologies – tapered tubes, nozzles, funnels, Y-junctions and multi-junctioned tubular structures – can be tuned a priori through gas phase chemistry. These morphologies exhibit thin walls (10–30 nm) and very larger internal diameters (up to 2.5 μm) suitable for micro-/nano-fluidic, drug delivery, and nanoelectronic applications. A mechanism governing the controlled growth of these new morphologies of carbon nanostructures is presented.

Typically, the growth of multi-walled carbon nanotubes is accomplished using transition metal catalysts such as nickel and iron.[13] During growth, the catalyst particle size and the growth interface do not change, thus maintaining a constant tube diameter. Controlling the morphology of the carbon nanostructures is of interest. Merkulov et al.,[14] used nickel catalyst and relative concentrations of C_2H_2/NH_3 to synthesize a "cylinder-on-cone" morphology. Again, the internal diameter of the structure is constant and determined by the nickel catalyst size. On the other hand, we hypothesized that the gallium meniscus with carbon in the absence or presence of oxygen or nitrogen would be different, similar to that of the dependence of contact angle on temperature. This variation of gallium meniscus shape with the growing "tube" will allow for tapering or curving of the growing carbon structures. In the presence of oxygen or nitrogen, gallium wets carbon,[15,16] thus forming a flatter meniscus during growth, see Figure 1 for the schematic. Based on this behavior of gallium we could successfully control and synthesize various morphologies of carbon nanostructures.

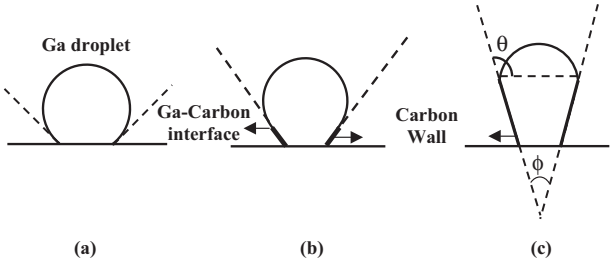

Fig. 1. Schematic of the growth mechanism. a) Initial gallium droplet, b) formation of carbon wall at the base of the gallium droplet. The wall forms tangential to the surface of the droplet. Addition of carbon occurs at the gallium carbon interface as shown. c) Geometric representation of the relation between the contact angle and the conical angle.

In the first set of experiments a film of gallium covered with molybdenum powder was exposed to 18 % CH_4/H_2 plasma for 1 h. These experiments resulted in hollow conical structures (cones and nozzles) of carbon with varying conical angles from 7° to 58° as shown in Figure 2.

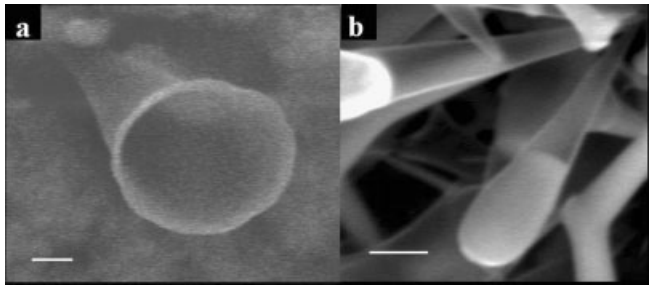

Fig. 2. Curved and tapered carbon tubular structures. Scanning electron microscopy (SEM) images of a) nozzles and b) cones synthesized upon exposing the prepared substrate to 18 % CH_4/H_2 plasma. Scale bar: a) 500 nm, b) 2 μm.

[*] Prof. M. K. Sunkara, G. Bhimarasetti
Department of Chemical Engineering, University of Louisville
Louisville, KY 40292 (USA)
E-mail: mahendra@louisville.edu
Dr. U. M. Graham, Dr. B. H. Davis
Center for Applied Energy Research, University of Kentucky
Lexington, KY 40511 (USA)
C. Suh, Prof. K. Rajan
Department of Materials Science and Engineering
Rensselaer Polytechnic Institute
Troy, NY 12180 (USA)

[**] Authors (G. B. and M. S.) acknowledge the support from National Science Foundation under CAREER program (CTS 9876251). K. R. and C. S. acknowledge the support from the National Science Foundation International Materials Institute program (DMR-0231291).

 DOI: 10.1002/adma.200305400

ADVANCED MATERIALS

A mechanism for the formation of varying conical angles of the carbon conical structures is described next. The presence of molybdenum promotes the nucleation of carbon at the gallium droplet–molybdenum interface and thus assists the formation of a carbon "tube" around the gallium droplet. As the carbon tube grows in length, the gallium–carbon interface (indicated in Fig. 1) lifts the gallium droplet by setting up a steady contact angle between the meniscus and the growing carbon wall, thus setting the tapering angle of the overall structure. During the initial stages of the growth process the system goes through certain unsteady state dynamics that gives rise to varying curvature at the base of the structures. The meniscus angle and the conical angle of the resulting carbon tube are related by the following relationship:

$$\phi = 2\theta - 180^\circ \quad (1)$$

where ϕ is the conical angle and θ is the contact angle between gallium and the developing interface (indicated in Fig. 1). Gao and Bando[11] showed that the contact angle of gallium inside a carbon tube with temperature up to 550 °C varies from 93° to 113°. Any differences in the temperature or the gas phase composition would change the contact angle and thus the meniscus angle. The tapering angles (or conical angles) of all structures synthesized in the absence of oxygen and nitrogen in the gas phase were in the range of 7–58°, corresponding to the estimated meniscus angles of 93–119° during growth, respectively.

The wetting behavior of gallium with carbon can be altered using the gas phase. In the presence of oxygen or nitrogen, gallium wets carbon more than it does in the absence of oxygen or nitrogen. Based on this, the next set of experiments were conducted by dosing the feed gases (CH_4 and H_2) with 5 sccm (standard cubic centimeter per minute) of oxygen. As per the hypothesis, these experiments resulted in straighter tubes with no or very small conical angles. These structures are shown in Figures 3a,b, illustrating that the conical angles of the structures can be controlled via the gas phase chemistry.

In order to control and alter the morphology of the structures during the growth process, we performed another set of experiments in which oxygen was introduced after 30 min of initial cone growth. Transmission electron microscopy (TEM) analysis of the resulting structures clearly showed a change in the shape of the structures along their length, as shown in Figure 3c. During the initial growth in the absence of oxygen conical structures are formed with a curved meniscus of gallium at the tip of the growing cones. When oxygen is introduced during the growth the meniscus flattens and further growth leads to a tube, thus forming a junction in one structure. Similarly, structures grown with a three step and six step sequences with oxygen "on/off" yielded carbon structures with built-in interfaces between different types of morphologies (cone and tube), as shown in Figure 3d,e. Another remarkable morphology was engineered by introducing oxygen at the start of the experiment for some time and later proceeding with no-oxygen. In the presence of oxygen a straighter tube forms, and in the subsequent step with no oxygen, further growth evolves into a cone. This sequence results

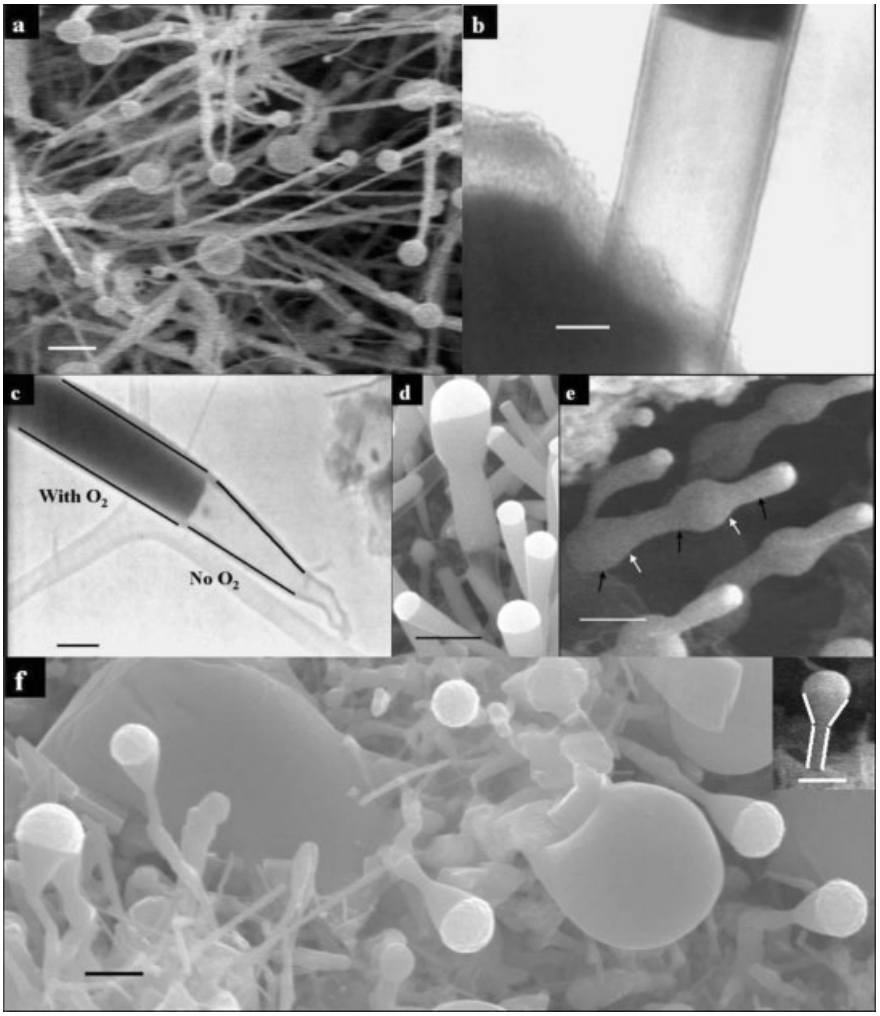

Fig. 3. Controlling the morphology via gas phase chemistry. a,b) SEM and bright-field TEM images of tubes grown by the addition of O_2 throughout the experiment. c) Bright-field TEM image of cone–tube morphology grown by no oxygen–oxygen sequence. d) SEM image of cone–tube–cone morphology grown by no oxygen–oxygen–no oxygen sequence. e) SEM image of the structure formed by 3 steps of oxygen-no oxygen sequence (total of 6 steps). Dark arrows show the part of the structure grown with no-oxygen and bright grown in the presence of oxygen. Tubular morphology in the first step is not seen in the figure. f) SEM image of the funnels grown by oxygen–no oxygen sequence. Inset shows a magnified SEM image of a funnel. Scale bar: a) 2 μm, b) 100 nm, c) 200 nm, d) 2 μm, e) 3 μm, and f) 1 μm, 1 μm (inset).

in the formation of a funnel (tube–cone) structure as shown in Figure 3f. In almost all the cases, an unsteady evolution of the carbon tube for approximately one diameter length (of the base diameter) is observed. Experiments with higher amounts of nitrogen (20 sccm compared to 5 sccm of O_2 in the previous experiments) produced conical structures that taper down with growth. These results illustrate that the meniscus angle could be less than 90° with increased nitrogen dissolution due to higher amounts of atomic nitrogen in the gas phase.

The physical impingement of two or more growing carbon structures with gallium at the tips would result in spontaneous coalescence of gallium droplets into one bigger droplet, due to strong cohesive forces associated with gallium. This type of coalescence, upon further growth, leads to the formation of seamless Y-junctions, as shown in Figures 4a,b. Theoretically, Y-junctions within carbon nanotubes were predicted to possess useful electronic junction properties.[17] Experimentally, till now, carbon tubular structures with Y-junctions were synthesized either by using a porous template for splitting the carbon nanostructure during growth,[18] or by branching during growth via pyrolysis.[19,20] Recently, "electron-beam welding" was used to create a Y-junction between two single walled carbon nanotubes.[21] The results presented in Figure 4 illustrate that one can reliably coalesce two or more independently growing tubes into one bigger tube during growth. The insert in Figure 4b furthermore indicates that even after two carbon tubular structures combine into a single tube, the entire channel way remains open.

The striking feature of these Y-junctions is that there is no blockage at Y-juncture point, as indicated by the TEM investigation. Also, the inner diameter of the bigger tube after junction is found to be equivalent to the diameter based on the volume generated from the two coalesced gallium droplets. These results further confirm the spontaneous coalescence of gallium droplets at tips of individual carbon tubular structures upon impingement while continuing growth in a normal fashion after coalescence. In addition, similar wall thickness is maintained even after coalescence. The size and openness of the channels make these multi-channeled carbon tubular structures promising for various micro-fluidic, micro-reactor, and electronic applications.

The carbon wall structure of all the synthesized structures (tube wall) is shown to be multi-walled and crystalline as illustrated in the high-resolution TEM (HRTEM) image in Figure 4c. The structures maintain a constant wall thickness throughout their length except at the tip. The wall thickness tapers only near the tip or the growth interface (Fig. 4d). This tapering of wall thickness at the growing tip is observed in almost all the samples examined using HRTEM. These results indicate that the wall is indeed growing tangential to the gallium meniscus, confirming the growth mechanism. The energy dispersive X-ray spectroscopy (EDS) analysis of gallium inside carbon tubular structures could not confirmatively resolve the presence of any molybdenum to the detection level. In any case, a thorough structural and compositional analysis of the walls using RAMAN spectroscopy and electron energy loss spectroscopy (EELS) is the subject of our on-going work.

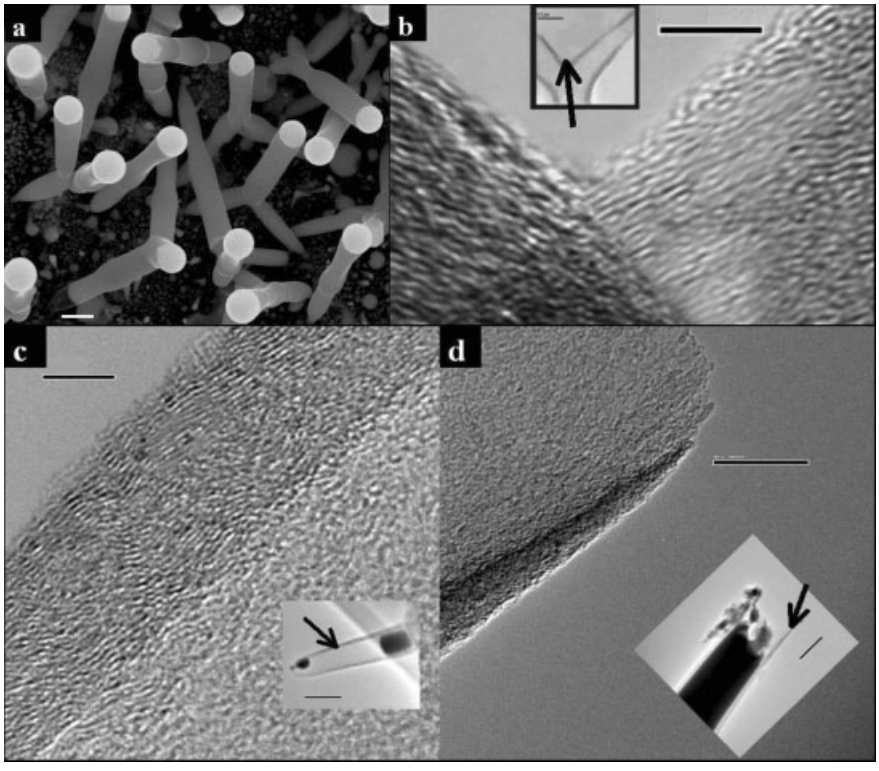

Fig. 4. Y-junctions and HRTEM images of the walls. a) SEM image of the Y-junctions formed by coalescence of gallium droplets at the tip of the growing structures. b) HRTEM image at the Y-junction. Inset shows the TEM of the Y-junction. c) HRTEM of the wall. Lattice fringes indicate graphitic structure of the walls. d) TEM image at the tip of the structure, indicating a tapering of the wall towards the tip. Scale bar: a) 2 μm, b) 5 nm, 200 nm (inset), c) 5 nm, 100 nm (inset), and d) 20 nm, 100 nm (inset).

In summary, we described a method to engineer, in a controlled manner, the morphology of carbon nanostructures, i.e., alter the shape of the growing carbon tubular structures in situ by changing the gas phase chemistry. Seamless Y-junctions with no internal obstructions can be reliably synthesized. It is also shown that one can produce junctions within one tube that lead to interconnected tubes or funnels or channel junctions. These multi-junctioned structures could find applications in nanoelectronic devices such as junction diodes. The synthesis of these nanostructures has implications in numerous materials science fields. One of these is the potential of using these large diameter tubular structures with no internal obstructions at channel junctions in mi-

ADVANCED MATERIALS

cro-fluidic applications as well as nanostructured percolation media. The hollow funnels can also serve as "nanocrucibles" for metal alloy production, which permit the containment and handling of very small amounts of metals. The latter would be of interest to the field of combinatorial synthesis, for instance, as potential micro/nano arrays for solid-state synthesis.

Experimental

The deposition experiments were conducted in an ASTeX 5010 Microwave Plasma reactor on various substrates including graphite, molybdenum, and titanium. A thin film of gallium is spread on the substrate. On top of the gallium film molybdenum powder purchased from Alfa Aesar (3–7 μm, 99.95 % purity) was dusted (1–15 % molybdenum to gallium atomic ratio). The setup was then exposed to 18 % CH_4/H_2 plasma at 1100 W microwave power and 40 torr reactor pressure for 1 h. The experiments were started by first striking the hydrogen plasma followed by introducing the methane gas. The experiments were shut down by turning off the methane gas followed by turning off the hydrogen gas supply. The heating of the substrate is solely due to the plasma, with no independent substrate heating. The temperature of the substrate was measured to be 800–850 °C by an optical pyrometer. Experiments to synthesize conical structures were performed using CH_4/H_2 only. In other experiments to control the morphology, the feed gases were dosed with 5 sccm of O_2 to 18 sccm of CH_4 and 100 sccm of H_2 at various stages of the growth process as required. For example, to synthesize funnels, oxygen was introduced right from the start of the experiment for about 30 min followed by turning off the oxygen gas supply. No other parameters were changed. The described structures were not observed on the as-synthesized samples. A layer of molybdenum–gallium alloy was observed as the top-most layer on the sample, which might have segregated during the shut down procedure. This could be avoided by temperature-controlled shut down, not possible with the reactor used. When the plasma is turned off, there is a sudden fluctuation in the temperature, as there is no substrate heating. This top layer was removed by gently tapping the sample, thus exposing the underneath carbon structures which are all over the substrate. The synthesized structures are analyzed using a JEOL JSM 5310 scanning electron microscope operated at 25 kV and a JEOL 2010F transmission electron microscope operated at 200 kV. For TEM analysis the structures formed on the substrate were transferred onto a holey carbon grid.

Received: May 15, 2003
Final version: July 8, 2003
Published online: August 25, 2003

[1] S. Iijima, *Nature* **1991**, *354*, 56.
[2] S. Amelinckx, X. B. Zhang, D. Bernaerts, X. F. Zhang, V. Ivanov, J. B. Nagy, *Science* **1994**, *265*, 635.
[3] A. Krishnan, E. Dujardin, M. M. J. Treacy, J. Hugdahl, S. Lynum, T. W. Ebbesen, *Nature* **1997**, *388*, 451.
[4] S. Iijima, M. Yudasaka, R. Yamada, S. Bandow, K. Suenaga, F. Kokai, K. Takahashi, *Chem. Phys. Lett.* **1999**, *309*, 165.
[5] Y. Gogotsi, J. A. Libera, N. Kalashnikov, M. Yoshimura, *Science* **2000**, *290*, 317.
[6] Y. Gogotsi, S. Dimovski, J. A. Libera, *Carbon* **2002**, *40*, 2263.
[7] P. M. Ajayan, J. M. Nugent, R. W. Siegel, B. Wei, P. Kohler-Redlich, *Nature* **2000**, *404*, 243.
[8] R. C. Mani, X. Li, M. K. Sunkara, K. Rajan, *Nano Lett.* **2003**, *3*, 671.
[9] J. Libera, Y. Gogotsi, *Carbon* **2001**, *39*, 1307.
[10] Y. Gao, Y. Bando, *Nature* **2002**, *415*, 599.
[11] Y. Gao, Y. Bando, *Appl. Phys. Lett.* **2002**, *81*, 3966.
[12] Z. W. Pan, S. Dai, D. B. Beach, N. D. Evans, D. H. Lowndes, *Appl. Phys. Lett*. **2003**, *82*, 1947.
[13] M. Meyyappan, L. Delzeit, A. Cassell, D. Hash, *Plasma Sources Sci. Technol*. **2003**, *12*, 205.
[14] V. I. Merkulov, M. A. Guillorn, D. H. Lowndes, M. L. Simpson, *Appl. Phys. Lett*. **2001**, *79*, 1178.
[15] S. Sharma, M. K. Sunkara, *J. Am. Chem. Soc.* **2002**, *124*, 12 288.
[16] U. H. Graham, S. Sharma, M. K. Sunkara, B. H. Davis, *Adv. Funct. Mater.* **2003**, *13,* 576.
[17] M. Menon, D. Srivastava, *Phys. Rev. Lett*. **1997**, *79*, 4453.
[18] J. Li, C. Papadopoulos, J. Xu, *Nature* **1999**, *402*, 253.
[19] W. Z. Li, J. G. Wen, Z. F. Ren, *Appl. Phys. Lett.* **2001**, *79*, 1879.
[20] B. C. Satishkumar, P. J. Thomas, A. Govindaraj, C. N. R. Rao, *Appl. Phys. Lett.* **2000**, *77*, 2530.
[21] M. Terrones, F. Banhart, N. Grobert, J. C. Charlier, H. Terrones, P. M. Ajayan, *Phys. Rev. Lett.* **2002**, *89*, 075 505.

30 nm Channel Length Pentacene Transistors**

By *Yuanjia Zhang*, *Jason R. Petta*, *Santha Ambily*, *Yulong Shen*, *Daniel C. Ralph*, and *George G. Malliaras**

Organic thin film transistors (OTFTs) are being developed for applications in smart tags and display drivers. Dramatic advances in the performance of organic semiconductors have been achieved in recent years and have brought their performance, in terms of field-effect mobility, to levels comparable with amorphous silicon.[1] A critical dimension in a TFT is the channel length L (the distance between the source and drain electrodes). Typically, transistors are fabricated with L of the order of tens of micrometers using optical lithography or by deposition through a stencil.[1] Studies of TFTs with much smaller L[2–11] have been motivated by the desire to increase both the device speed and the saturation current, the highest current that the transistor delivers at a given gate voltage.

As early as 1987, Turner-Jones et al. demonstrated an organic transistor with a 50 nm channel length, which was defined by using shadowed deposition of Au on a tilted substrate.[2] The transistor worked in the electrochemical mode, i.e., by modulation of the conductivity of polyaniline through electrochemical doping/dedoping. In 1993, Franssila et al. demonstrated the first sub-100 nm organic field-effect transistor.[3] Anisotropic etching was used to fabricate nanoscale oxide pillars that served as the lift-off masks for defining the channel. Solution-coated polythiophene was used as the semiconductor. However, the characteristics of the transistors were poor, exhibiting only minor gating effects.

More recently, Collet et al. used electron beam lithography to define channels as small as 30 nm.[4,7,8] The channels were fabricated directly on top of evaporated films of small molecules such as sexithiophene. Rogers et al. combined near-field photolithography with microcontact printing and shadow masking to demonstrate complementary inverter circuits from organic transistors with $L = 100$ nm.[5] A phthalocyanine and

[*] Prof. G. G. Malliaras, Y. Zhang, Dr. S. Ambily, Y. Shen
Department of Materials Science and Engineering
Cornell University
Ithaca, NY 14853-1501 (USA)
E-mail: george@ccmr.cornell.edu
Prof. D. C. Ralph, Dr. J. R. Petta
Laboratory of Atomic and Solid State Physics
Cornell University
Ithaca, NY 14853-2501 (USA)

[**] This work was supported primarily by the Nanoscale Science and Engineering Initiative of the National Science Foundation under NSF Award Number EEC-0117770, with additional support from NSF DMR-0071631 and DARPA. A portion of this work was conducted at the Cornell Nanofabrication Facility (a member of the National Nanofabrication Users Network) which is supported by the National Science Foundation under Grant ECS-9731293.

  DOI: 10.1002/adma.200305158